Cogn Neurodyn (2015) 9:129–144
DOI 10.1007/s11571-014-9311-3

RESEARCH ARTICLE

Energy coding in neural network with inhibitory neurons

Ziyin Wang · Rubin Wang · Ruiyan Fang

Received: 18 July 2014 / Revised: 1 September 2014 / Accepted: 6 September 2014 / Published online: 1 October 2014

Abstract This paper aimed at assessing and comparing the effects of the inhibitory neurons in the neural network on the neural energy distribution, and the network activities in the absence of the inhibitory neurons to understand the nature of neural energy distribution and neural energy coding. Stimulus, synchronous oscillation has significant difference between neural networks with and without inhibitory neurons, and this difference can be quantitatively evaluated by the characteristic energy distribution. In addition, the synchronous oscillation difference of the neural activity can be quantitatively described by change of the energy distribution if the network parameters are gradually adjusted. Compared with traditional method of correlation coefficient analysis, the quantitative indicators based on nervous energy distribution characteristics are more effective in reflecting the dynamic features of the neural network activities. Meanwhile, this neural coding method from a global perspective of neural activity effectively avoids the current defects of neural encoding and decoding theory and enormous difficulties encountered. Our studies have shown that neural energy coding is a new coding theory with high efficiency and great potential.

Keywords Neural coding · Neural energy · Inhibitory neurons

Z. Wang · R. Wang (✉) · R. Fang
Institute for Cognitive Neurodynamics, School of Science, East China University of Science and Technology, Shanghai 200237, China
e-mail: rbwang@ecust.edu.cn

Introduction

Neural information encoding and decoding is one of the core areas of research in neuroscience (Borst and Theunissen 1999; Gazzaniga et al. 2009; Jacobs et al. 2009). Currently, the main coding technologies include perceptual coding, phase coding, frequency coding and population coding etc. (Johnson 2004; Nirenberg and Latham 2003; Victor 1999; Rokem et al. 2006; Liu et al. 2010; Xie and Wang 2013; Pakhomov and Sudin 2013). However, these neural coding theories have many difficulties in studying neural encoding and decoding in the brain (McLaughlin 2009; Gopathy Purushothanman & David 2005).The main reason is that these coding theories are local and regional, and do not cross influence of large-scale neurological activities. Meanwhile, there is a paucity of adequate data analysis for resolving this issue (Simon 2003; Wang and Zhang 2006; Wang and Wang 2004), which is mainly due to limitations of experimental neuroscience and technology, i.e. the current experimental equipment are unable to simultaneously record massive and large-scale neural network activities. Another reason is that most models based on H–H equation need numerous computing resources, especially in simulating activities of large neuronal population (Feldman 2013).

Regarding the above-mentioned two difficulties, a hypothesis on the energy dynamics has been postulated to elucidate the theory of neural coding, about which a series of research results can be found in published literature. (Wang and Zhang 2006; Wang et al. 2009, 2008; Wang and Zhang 2012, 2007). These results not only present the energy formula for a single neuron (Wang et al. 2009; Wang and Zhang 2007), but also describe the energy distribution characteristics and energy coding in structural neural networks (Wang and Wang 2004). Important findings suggest that: (1) the

theory of neural energy coding is based on the use of a global concept of energy (2) the neurons release their stored energy within a very short time (negative energy) at the beginning of firing action potential, after which the oxyhemoglobin provides them with biological energy (Wang et al. 2004), and this mechanism contradicts the traditional theory of pure energy consumption in neurons, (3) the distribution of the negative energy, as assessed by parameter studies reflect the neural network parameters and neural oscillation with a high consistency; and thus, laid the foundation for energy coding research in functional neural network (Wang and Wang 2004).

Among others, the Wang et al. study reported their detailed observations on the energy distribution and energy coding of a structural neural network; however, this study considered only the excitatory neurons. Original meaning is that the study in ref (Wang and Wang 2004) studied an extensively neural work that considered only excitatory neurons. Although neural networks have been extensively reported in published literature, this study considered only excitatory neurons. Based on research in neurophysiology, most of the functional neural networks contain about 20 % of inhibitory neurons (Nicholls et al. 2001), and significantly contribute towards modulating neuronal network activity and neural coding (Sokoloff 2008; Moore and Cao 2008). Therefore, this paper aimed at systematically exploring the effects of the inhibitory neurons in the neural network on the neural energy distribution, and compared the network activities in the absence of the inhibitory neurons, so as to understand the nature of neural energy distribution and neural energy coding, which can serve as a basis for future studies on energy coding in functional neural networks.

Biophysical model

The model proposed by Wang et al. (2009) was considered as a basis for the development of this novel biophysical model of a neuron, in order to simulate the energy coding in neuronal network.

Compared to the typical model of a single neuron, an additional voltage source, current source, and inductor are included into the mth model (Fig. 1). The differences in the concentration of various ions inside and outside the neuron, drives the ions to move, and thus, becomes a source of voltage. A neuron accepts the stimulation from the peripheral neurons with the development of the ionic gradient, leading to the flow of voltage-gated current. Moreover, the influx and release of charged ions (K^+, Na^+, Ca^{2+}) from the channels results in the formation of a self-induced current loop, which is equivalent to an inductance element. In the figure, for the convergence of positive and negative ions, inside and outside the cellular membrane, C_m and I_m denotes the membranous capacitance and total electric current of stimulation, when stimulation of N neurons acts on the mth neuron, respectively. To account for loss in the non-ideal current source and voltage source, r_m and $r_{0m}$are use to describe the resistance across I_m and U, respectively. Because the current source and the voltage source were not acting in the same position, the film resistor was divided into three parts, denoted by r_{1m}, r_{2m} and r_{3m}. The following coupling relation describes the sum of the input current and connected neurons:

$$I_m = i_{1m} + \sum_{j=1}^{n}\left[i_{om}(j-1)\sin\left(\omega_m(j-1)\left(t_j - t_{j-1}\right)\right)\right] + i_{0m}(n)sin(\omega_m(n)(t-t_n)) \quad (1)$$

where i_{1m} is current for maintenance of the resting membrane potential, i_{0m} is the total effect generated by the current stimulation of peripheral neurons, ω_m is the firing frequency.The circuit equations, corresponding to Fig. 1, are

$$\begin{cases} U_m = r_{0m}I_{0m} + r_{1m}I_{1m} + L_m\dot{I}_{1m} \\ I_{0m} = I_{1m} - I_m + \dfrac{U_{im}}{r_m} + C_m\dot{U}_{1m} \\ U_{im} = C_m r_{3m}\dot{U}_{0m} + U_{0m} \end{cases} \quad (2)$$

$$L_m\dot{I}_{1m} + r_{1m}I_m = K_{1m}\dot{U}_{0m} + K_{2m}U_{0m} - r_{2m}I_m \quad (3)$$

where $K_{1m} = C_m(r_{2m} + r_{3m} + \frac{r_{2m}r_{3m}}{r_m}), K_{2m} = 1 + \frac{r_{2m}}{r_m}$. The total power consumed by the neural network composed of N such neurons is as follows:

$$P_m = d_{1m}\dot{U}_{0m}^2 + d_{2m}\dot{U}_{0m} + d_{3m}\dot{U}_{0m}U_{0m} + d_{4m}U_{0m}^2 + d_{5m}U_{0m} + d_{6m} \quad (4)$$

where,

$$d_{1m} = C_m^2\left(1 + \frac{r_{3m}}{r_m}\right)\left(r_{0m} + r_{2m} + r_{3m} + \frac{r_{3m}(r_{0m} + r_{2m})}{r_m}\right)$$

$$d_{2m} = C_m\left[\left(2r_{0m} + r_{2m} + r_{3m} + \frac{2r_{0m}r_{3m} + r_{2m}r_{3m}}{r_m}\right)\cdot\left(Ke^{-at} - \frac{r_{2m}}{L_m}e^{-at}\int_{t_0}^{t} I_m e^{at}dt\right) - 2\left(1 + \frac{r_{3m}}{r_m}\right)(r_{0m} + r_{2m})I_m\right]$$

$$d_{3m} = C_m\left[r_{0m}\left(1 + \frac{r_{3m}}{r_m}\right)\frac{2(r_m + r_{1m} + r_{2m})}{r_m r_{1m}} + \frac{1}{r_m^2}\left(r_m^2 + 2(r_m r_{2m} + r_m r_{3m} + r_{2m}r_{3m}) + \frac{(r_m + r_{2m})(r_m r_{2m} + r_m r_{3m} + r_{2m}r_{3m})}{r_{1m}}\right)\right]$$

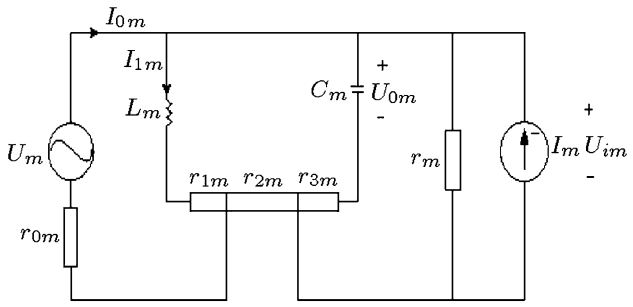

Fig. 1 Physical model of mth neuron

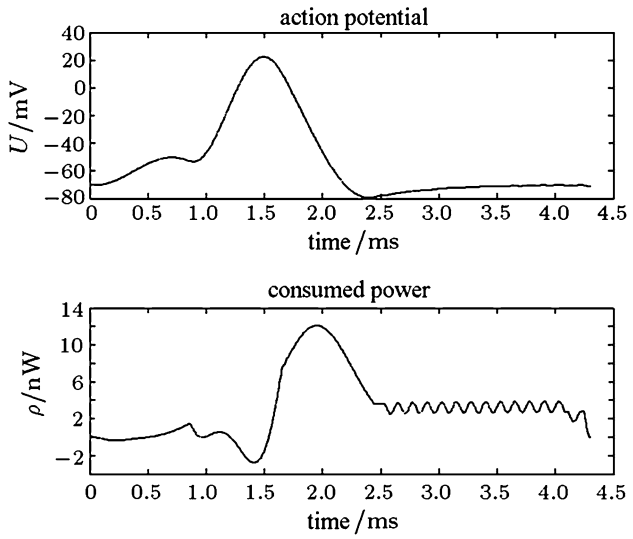

Fig. 2 Action potential and corresponding power function

$$d_{4m} = \frac{1}{r_m^2}\left(1+\frac{r_m+r_{2m}}{r_{1m}}\right)\cdot\left(r_{0m}\left(1+\frac{r_m+r_{2m}}{r_{1m}}\right)+r_m+r_{2m}\right)$$

$$d_{5m} = \frac{2r_{0m}(r_m+r_{1m}+r_{2m})+r_{1m}(r_m+2r_{1m}+r_{2m})+r_m r_{1m}}{r_m r_{1m}}\left(Ke^{-at}-\frac{r_{2m}}{L_m}e^{-at}\int_{t_0}^{t} I_m e^{at}dt\right) - \frac{2r_{0m}(r_m+r_{1m}+r_{2m})+r_{2m}(r_m+2r_{1m}+r_{2m})+r_m r_{1m}}{r_m r_{1m}}\cdot I_m$$

$$d_{6m} = \left[r_{0m}\left(Ke^{-at}-\frac{r_{2m}}{L_m}e^{-at}\int_{t_0}^{t} I_m e^{at}dt\right)-(r_{0m}+r_{2m})I_m\right]\cdot\left[Ke^{-at}-\frac{r_{2m}}{L_m}e^{-at}\int_{t_0}^{t} I_m e^{at}dt - I_m\right]$$

According to principles of physics, power is the average energy in unit time. In this paper, energy indicates power, unless otherwise indicated. Equations (2)–(5) indicate the exact solution of the membrane potential:

$$U_{0m} = -\frac{\hat{g}_1}{\lambda_m^2}-\frac{\hat{g}_2 e^{-a(t-t_n)}}{\lambda_m^2-a^2}-\frac{1}{\lambda_m^2+\omega_m^2}(\hat{g}_3\sin(\omega_m(n)(t-t_n)) + \hat{g}_4 cos(\omega_m(n)(t-t_n))) \times\left(U_{0m}(t_n)+\frac{\hat{g}_1}{\lambda_m^2}+\frac{\hat{g}_2}{\lambda_m^2-a^2}+\frac{\hat{g}_4}{\lambda_m^2+\omega_m^2(n)}\right)e^{-\lambda_m(t-t_n)} \quad (5)$$

Equation (5) computes the action potential obtained by energy method, and its numerical solution is presented in the upper plot in Fig. 2. Substituting Eq. (5) into the neuron's power Eq. (4), the power function obtained is illustrated in the lower plot in Fig. 2.

Figure 2 suggests that this novel biophysical model can effectively simulate the firing of the action potential in neurons, wherein the peak of the power consumption curve lags behind that of the membrane potential, which is due to the inertia of capacitance elements and inductance in the model. Detailed discussions about various circuit elements in the biophysical model and the solution process is mentioned elsewhere in published literature (Wang et al. 2009; Wang and Zhang 2007).

The positive and negative regions in the power curve significantly affect neurobiology. It explains the reason for a very slight increase of oxygen consumption, with a substantial increase in cerebral blood flow as neurons in the brain are activated; a neurophysiological phenomenon that was not clear until now (Sokoloff 2008; Moore and Cao 2008; Lin et al. 2010). It also explains the reason for a synchronous effect between external stimuli and perception, which is still unexplained in cognitive neuroscience (Wang and Zhang 2012; Dhamala et al. 2004).

Structural neural network model

The assumed connection structure in cortical neural network is as shown in Fig. 3, which shows a coupling between each neuron in the network. Each neuron was simulated based on the biophysical model shown in Fig. 1. Therefore, the following neural network structure conforms with the specified limits of neurobiology (Wang and Zhang 2006; Wang et al. 2009).

The neural network in Fig. 3 is composed of 15 fully connected neurons. Due to the high complexity of cortical neuronal connections, the average number of peripheral neurons connected to any neuron was around 10^4 (Chadderton et al. 2014; Igarashi et al. 2007). The purpose of this paper was to explore the energy coding pattern of the neural

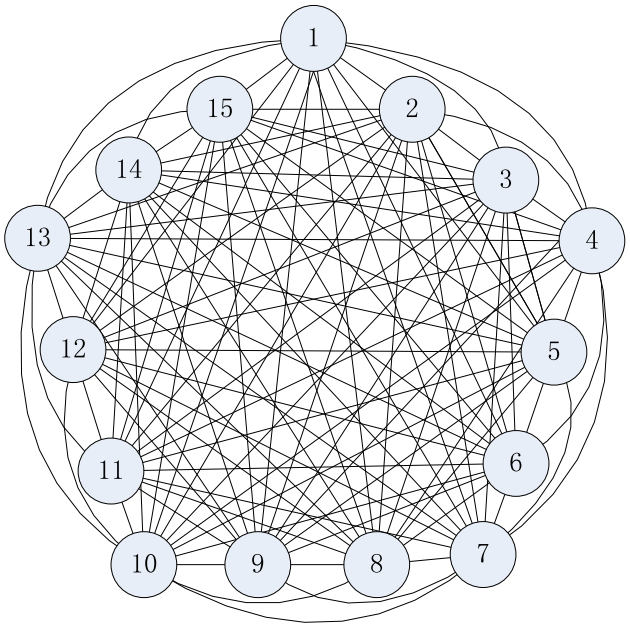

Fig. 3 Connection structure of neural network

network when stimulated, and hence, we adopted some simple connections in the neural network. A line between two neurons denotes coupling and a two-way connection. Coupling strength varied between any two neurons, and the coupling between two neurons was asymmetric as well. For example, the coupling strength from the first neuron to the second was 0.15, while that from the second neuron to the first was 0.22. Statistically, the range of the synaptic coupling strength between neurons is a random value with uniform distribution (Wang and Wang 2004). Based on data from published literature, we assumed that the value ranged between 0.1 and 0.3 (Rubinov et al. 2011).

The coupling strength of the matrix was as follows: $\mathrm{W} = \begin{bmatrix} w_{1,1} & \cdots & w_{1,n} \\ \vdots & \ddots & \vdots \\ w_{n,1} & \cdots & w_{n,n} \end{bmatrix}$ where, $w_{i,j}$ represented the coupling strength between the ith and jth neurons.

The operating manner of the network was as follows:

1.

$$\begin{aligned} I_{interneuron}(t) &= W \times Q(t-\tau)^T \\ I(t) &= I_{interneuron}(t) + I_{external}(t) \\ S_j(t) &= \frac{\tau}{t}\big(I(t) - S_j(t-\tau)\big) + S_j(t-\tau) \end{aligned} \tag{6}$$

2.

$$I_{m,j}(t) = \begin{cases} i_{ml} + \sum_{j=1}^{n}\left[i_{0m}(j-1)\sin\big(\omega_m(j-1)\big(t_j - t_{j-1}\big)\big)\right] + \\ i_{0m}(n)\sin(\omega_m(n)(t-t_n)), \quad \text{if } S_j(t) > th \\ i_{ml}, \qquad\qquad \text{if} S_j(t) < th \end{cases} \tag{7}$$

3. By substituting Eq. (3) in Eq. (5), we obtained the membrane potential $U_{0m,j}(t)$.
4. Substituting the results of Eq. (5) in Eq. (4), we obtained the total power consumption $P_{m,j}(t)$

where $S_j(t)$ is the total stimulation of the jth neuron at time t, and $Q(t-\tau) = [Q_1(t-\tau), Q_2(t-\tau), \ldots\ldots Q_j(t-\tau), \ldots Q_n(t-\tau)]$ indicates the firing states of the neurons, with a resting value of 0 and firing value of 1.

Characteristics of total power consumption of network with oscillation in different parameters

Characteristics of power consumption in neuronal population with continuous stimulation

We adopted a neuronal population model consisting of 15 neurons. In order to cover the entire mammalian brain, we selected the ratio of excitatory neurons to inhibitory neurons as 4:1 (Nicholls et al. 2001). We selected the neurons from fifth until seventh as the inhibitory neurons, and the rest as the excitatory neurons. We continuously stimulated the first and second neurons with an intensity of 40 mV and successfully stimulated n number of neurons, where n was the number of neurons in the neural network. The coupling strengths between excitatory neurons and inhibitory neurons accord were uniformly distributed at the [0, a] and [0, $2a$], respectively, while the excitation delivery time depended on the uniform distribution [0.5 ms, 1.5 ms]. From the nerve impulse record, the total power consumption of the network was as shown in Fig. 4. In Fig. 4a, when the neuron j fires at time t, a black marker is recorded at *(t, j)*.

In Fig. 4a, continuous stimulations were applied to the first and second neurons, indicating that they maintained releasing pulses cyclically after their first firing potential. Due to their excitability, the high frequency firings accelerated the ascendance of membrane potential in other neurons. In addition to these two neurons applied by continuous stimulation, the firing of other neurons was irregular, because of which the total power consumption over time in the neural network also fluctuated, which is shown in Fig. 4c.

As seen from Fig. 4b, a significant periodicity was observed in the firing of the neurons in the neural network, and this corresponds to the total power consumption (Fig. 4d). Comparing results for Fig. 4b and d, we observed that the neurons in a network without inhibitory neurons show higher firing frequency. This is because once a neuron fires an action potential, it will produce stimulate other neurons, resulting in a rapid increase in their membrane potentials after the refractory period, and

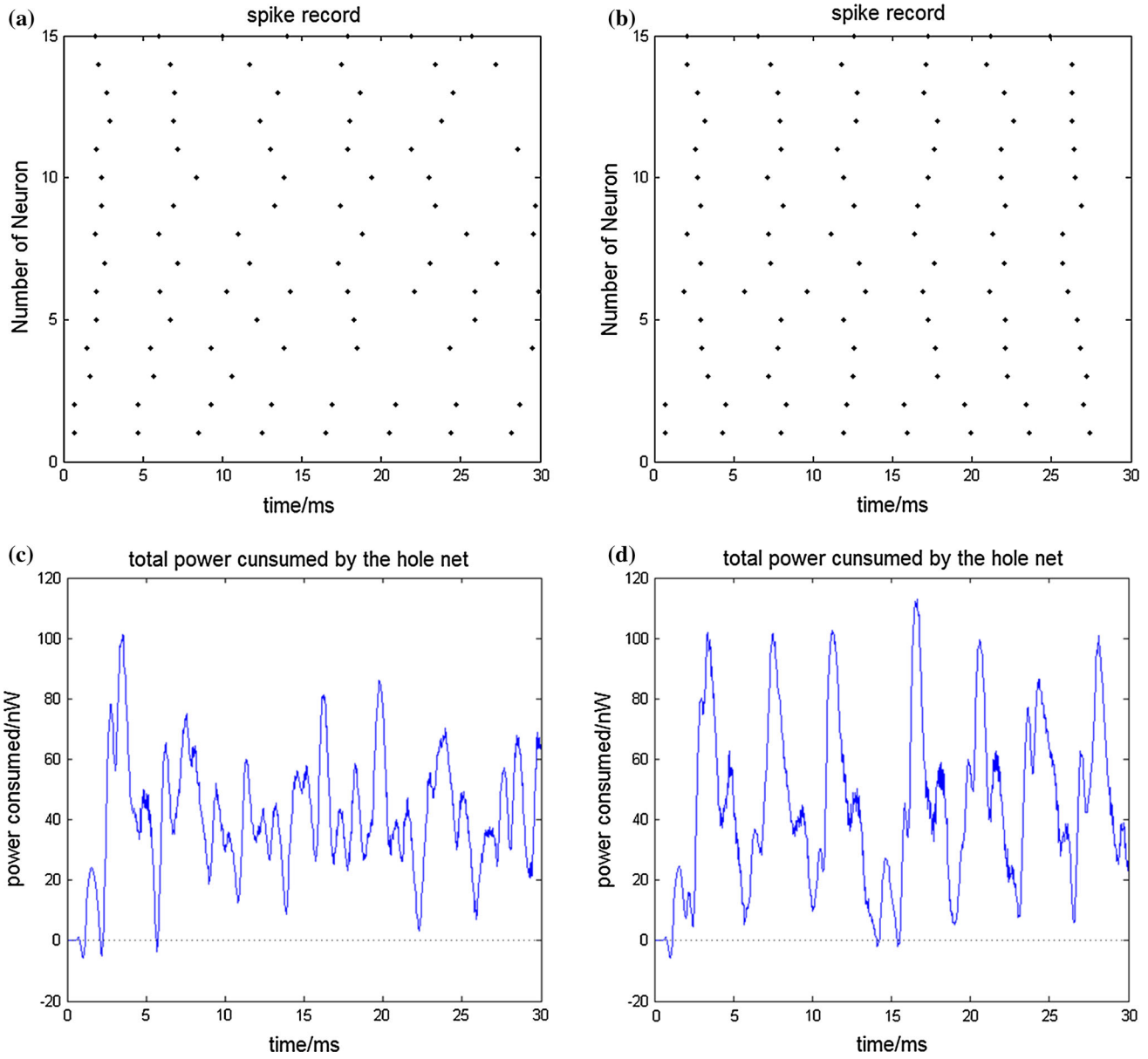

Fig. 4 **a** Nerve impulse record of continuous simulation (with inhibitory neurons) of network with 15 neurons. **b** Nerve impulse record of continuous simulation (without inhibitory neurons) of network with 15 neurons. **c** Total power consumption of the network with continuous stimulation (with inhibitory neurons). **d** Total power consumption of the network with continuous stimulation (without inhibitory neurons). $a = 0.5 + 0.5 \times \frac{10}{n}$, Coupling strengths between excitatory neurons and those between inhibitory neurons accorded with uniform distribution on the [0, a] and [0, 2a], respectively, while the excitation delivery time was uniformly distributed at [0.5 ms, 1.5 ms]

consequently, issue action potentials upon reaching the threshold. On the other hand, pulse firings of the inhibitory neurons will reduce the membrane potentials of other neurons to some extent and decline the overall firing frequency of neurons, which leads to a lower power consumption in the neural network. In other words, neural activity differences in the network caused by presence or absence of the inhibitory neurons can be detected by the nervous energy produced.

Correlation coefficient can be used to characterize synchronization of neural oscillations. However, for assessment of energy, a more concise and effective quantitative computation method, named negative energy ratio, was proposed and studied (Wang and Wang 2004), which is more effective in analyzing neural oscillation differences caused by different network parameters.

In a neural network consisting of n neurons, we can obtain a symmetric matrix of correlation coefficient. If the

matrix elements C, and C_{ij}, denoted as the elements in the *ith* row and *jth* column, then C_{ij} denotes the correlation coefficient of membrane potentials between the *ith* and *jth* neurons. Our previous studies have shown that if the network can obtain synchronization after instant stimulation, two or more oscillation groups will appear in the steady state. The firing of the first group stimulates neuron firings in other groups. However, due to a delay in signal transmission (Haken 2007; Ghosh et al. 2008), the other groups will receive stimulation and fire energy after a lag. At this time, the firing in the first group would have stopped, and it would be stimulated by the firings from other groups, forming coupled oscillations. This indicates that the most significant synchronization will occur inside an oscillation group. Normally, the correlation coefficient between the membrane potential of a neuron and those of other $n-1$ neurons are different. We select the maximum correlation coefficient (divided by correlation coefficient of membrane potential $C_{ii}=1$) to characterize neuronal synchronization with the host group, denoted as ρ^{i}_{max} Thus, the synchronization of the entire network can be characterized by taking the average value of the maximum correlation coefficients.

The average of maximum correlation coefficient is defined as:

$$\rho_{mean}=\frac{\sum_{i=1}^{n} max(C_{i,1},C_{i,2},\cdots C_{i,j},\cdots,C_{i,n})}{n}(i\neq j) \quad (8)$$

where $C_{i,j}$ is the correlation coefficient between neuron and membrane potential, and it is given by:

$$C_{i,j}=\frac{\sum_{k=1}^{T/\Delta t}|(V_i(k\Delta t)-\bar{V}_i)||(V_j(k\Delta t)-\bar{V}_j)|}{\sqrt{\sum_{k=1}^{T/\Delta t}(V_i(k\Delta t)-\bar{V}_i)^2(V_j(k\Delta t)-\bar{V}_j)^2}} \quad (9)$$

It should be noted that the simulated membrane potential is a discrete time sequence. In Eq. (9), Δt is the sampling interval, and $\bar{V}_i$ represents the mean value of membrane potential sequence of the *ith* neuron. We may see that if the correlation coefficients between any two neurons are closer to 1, it indicates a higher synchronization between them.

Negative energy ratio is defined as the ratio of absolute value of the negative energy consumed by neuronal population from time 0 to time t, over the sum of absolute values of positive and negative energies, that is:

$$\alpha(t)=\frac{E_{negative}}{E_{negative}+E_{positive}}\times 100\% \quad (10)$$

$$E_{negative}=\sum_{i=1}^{n}\int_{0}^{t}P_i(t)\times sgn(-P_i(t))dt \quad (11)$$

$$E_{positive}\sum_{i=1}^{n}\int_{0}^{t}P_i(t)\times sgn(P_i(t))dt \quad (12)$$

where $P_i(t)$ was the power consumed by neurons at time t, and its integration on $[0, t]$ means the power consumed during a time of $[0, t]$. While $sgn(\cdot)$ is a sign function defined as: $sgn(x)=\begin{cases}1, & x<0\\ 0, & x\geq 0\end{cases}$

Based on the results in Fig. 4, we increased the number of neurons in the network. In a neuronal population network consisting of n neurons, we randomly selected $5/n$ neurons as inhibitory neurons. Continuous stimulations are applied to any number of excitatory neurons at time $t=0$, with stimulation intensity of *40* mV. Among these, the coupling strengths between excitatory neurons and those between inhibitory neurons accord with uniform distribution on the $[0, a]$ and $[0, 2a]$, respectively, while the excitation delivery time was uniformly distributed on [0.5 ms, 1.5 ms].

Figure 5a–d represent the nerve impulse firings within 30 ms in the entire network consisting of 30, 50, 100 and 500 neurons, respectively, and their total power consumption curves over time are shown in Fig. 6a–d.

In a neural network consisting of 30 neurons shown in Fig. 5a, the obvious regularity of the overall firing of the network was not observed, synchronization of overall firing of the network consisting of 100 neurons was observed, as shown in Fig. 5c, and the synchronization was very significant in a network consisting of 500 neurons, as shown in Fig. 5d.

Correspondingly, the coupling strength distribution remained within a network with inhibitory neurons, (Fig. 6). As the number of neurons in the neuronal population increased, the periodic trends of the total power consumption become apparent, and even appeared to be negative power. Thus, we concluded that the neural activity difference in the network was dependent on the quantity of neurons, and probably reflected through nervous energy. Table 1 lists the negative energy ratio and the average of maximum correlation coefficients corresponding to results in Fig. 6.

From results in Figs. 5, 6. and Table 1, the ribbon pattern of the nerve impulse record become apparent with an increase in the quantity of neurons, indicating that synchronization in the oscillatory process gradually strengthens, thereby allowing the accords with an increased average of maximum correlation coefficients (Table 1). Additionally, the proportion of negative energy shows that the same monotonicity with a gradual increase in the number of neurons. Meanwhile, the distribution characteristics of the total power consumption were also closely related to network synchronization. The results in Table 1 indicate that this relation is monotonous, which means that the higher the number of neurons in a coupled neuronal network, the easier it is for the

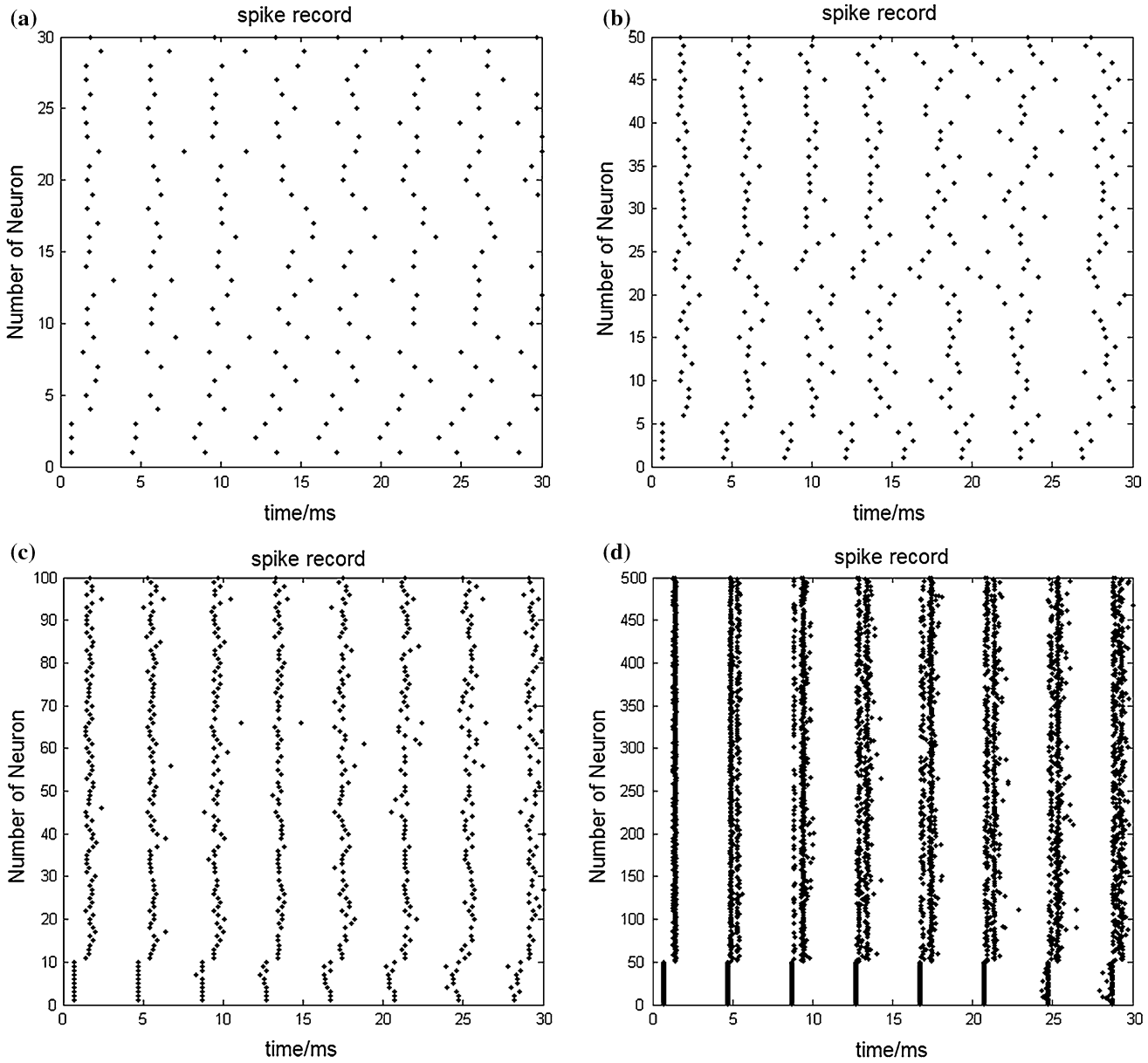

Fig. 5 **a** Nerve impulse record of 30 neurons. **b** Nerve impulse record of 50 neurons. **c** Nerve impulse record of 100 neurons. **d** Nerve impulse record of 500 neurons. $a = 0.5 + 0.5 \times \frac{10}{n}$, Coupling strengths between excitatory neurons and those between inhibitory neurons accorded with uniform distribution on the [0, a] and [0, $2a$], respectively, while the excitation delivery time was uniformly distributed at [0.5 ms, 1.5 ms]

network to enter the synchronized state with continuous stimulation, with a higher proportion of negative energy in the total energy (energy is obtained by integrating power, which can be characterized by area between power curve and the axis).

In order to have a more intuitive understanding of inhibitory neurons' effect on the neuronal network, we conducted simulations to compare the performances of neuronal network consisting of various neurons in the presence and absence of inhibitory neurons. In a neuronal population model consisting of n neurons, we randomly selected $n/5$ neurons as inhibitory neurons. Continuous stimulations were applied to any number of excitatory neurons at time $t = 0$ with stimulation intensity of 40 mV, where the coupling strengths between excitatory neurons and those between inhibitory neurons accord with uniform distribution on the [0, a] and [0, a], respectively, while the excitation delivery time was uniformly distributed at [0.5 ms, 1.5 ms].

Figure 7 shows the impulse firing and Fig. 8 shows the corresponding total power consumption in the neuronal network within 30 ms by simulation.

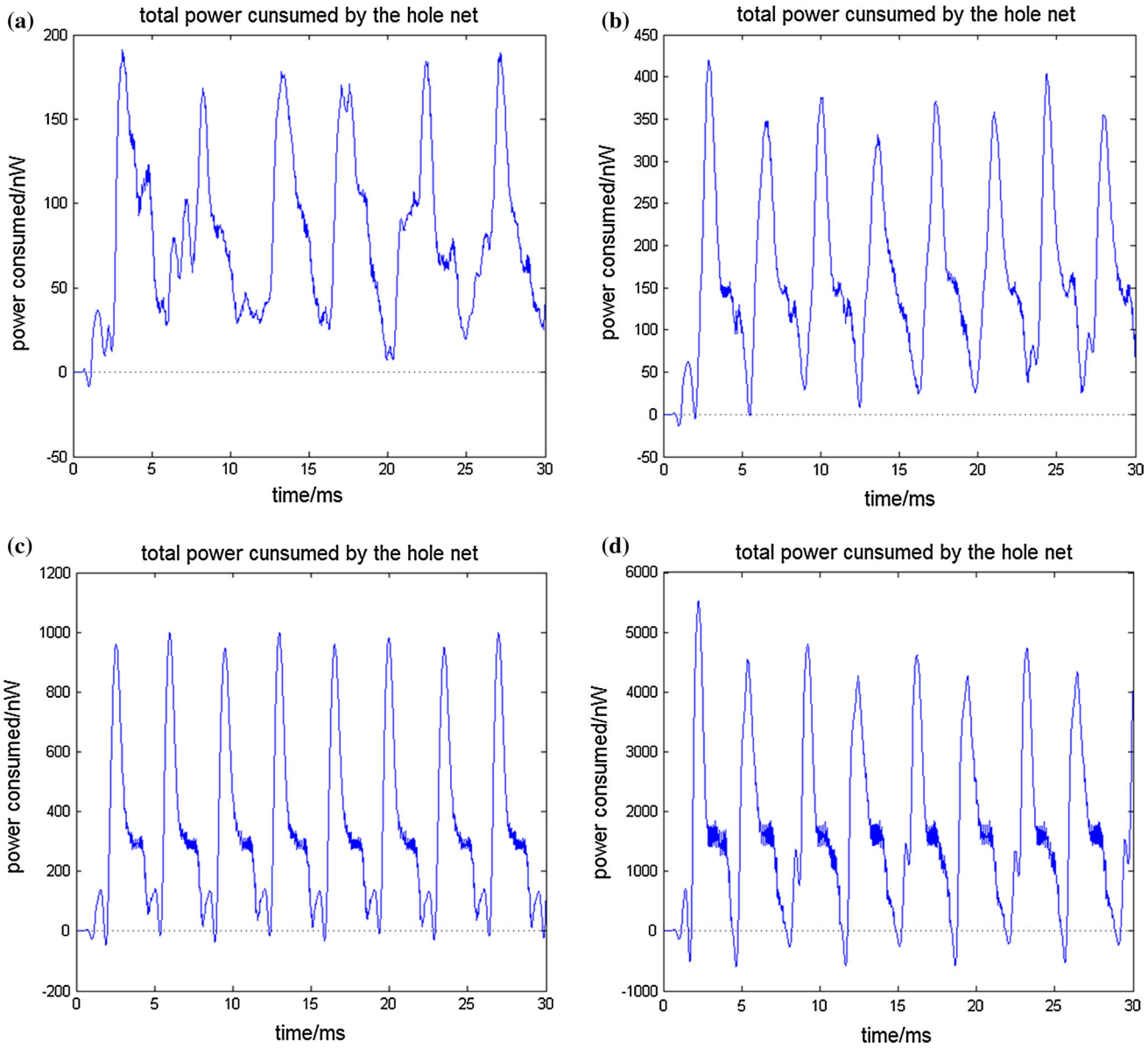

Fig. 6 **a** Total power consumption of 30 neurons. **b** Total power consumption of 50 neurons. **c** Total power consumption of 100 neurons. **d** Total power consumption of 500 neurons. $a = 0.5 + 0.5 \times \frac{10}{n}$, Coupling strengths between excitatory neurons and those between inhibitory neurons accorded with uniform distribution on the [0, a] and [0, $2a$], respectively, while the excitation delivery time was uniformly distributed at [0.5 ms, 1.5 ms]

Table 1 Negative energy ratio and average of maximum correlation coefficient corresponding to neuronal network in Fig. 6

Number of neurons	30	50	100	500
Negative energy ratio α (t) (%)	0.0511	0.0569	0.0668	1.3970
Average of maximum correlation coefficient ρ_{mean}	0.5678	0.6779	0.8460	0.9026

Coupling strengths between excitatory neurons and those between inhibitory neurons accord with uniform distribution on the [0, a] and [0, $2a$], respectively, while the excitation delivery time is uniformly distributed on [0.5 ms, 1.5 ms]

From Fig. 7, we clearly observe that the impulse firing of neurons have stronger synchronization with the absence of the inhibitory neurons in the neural network. Comparing the results in Fig. 7c and g, dots in (g) are more concentrated in the longitudinal straight line, appearing thinner and smoother, while some dots in (c) scatter out of the line, appearing a certain fluctuation in the transverse direction. Comparing total power consumption curves in networks with the same number of neurons and with the presence or absence of inhibitory neurons, we found that inhibitory neurons can significantly reduce the negative energy,

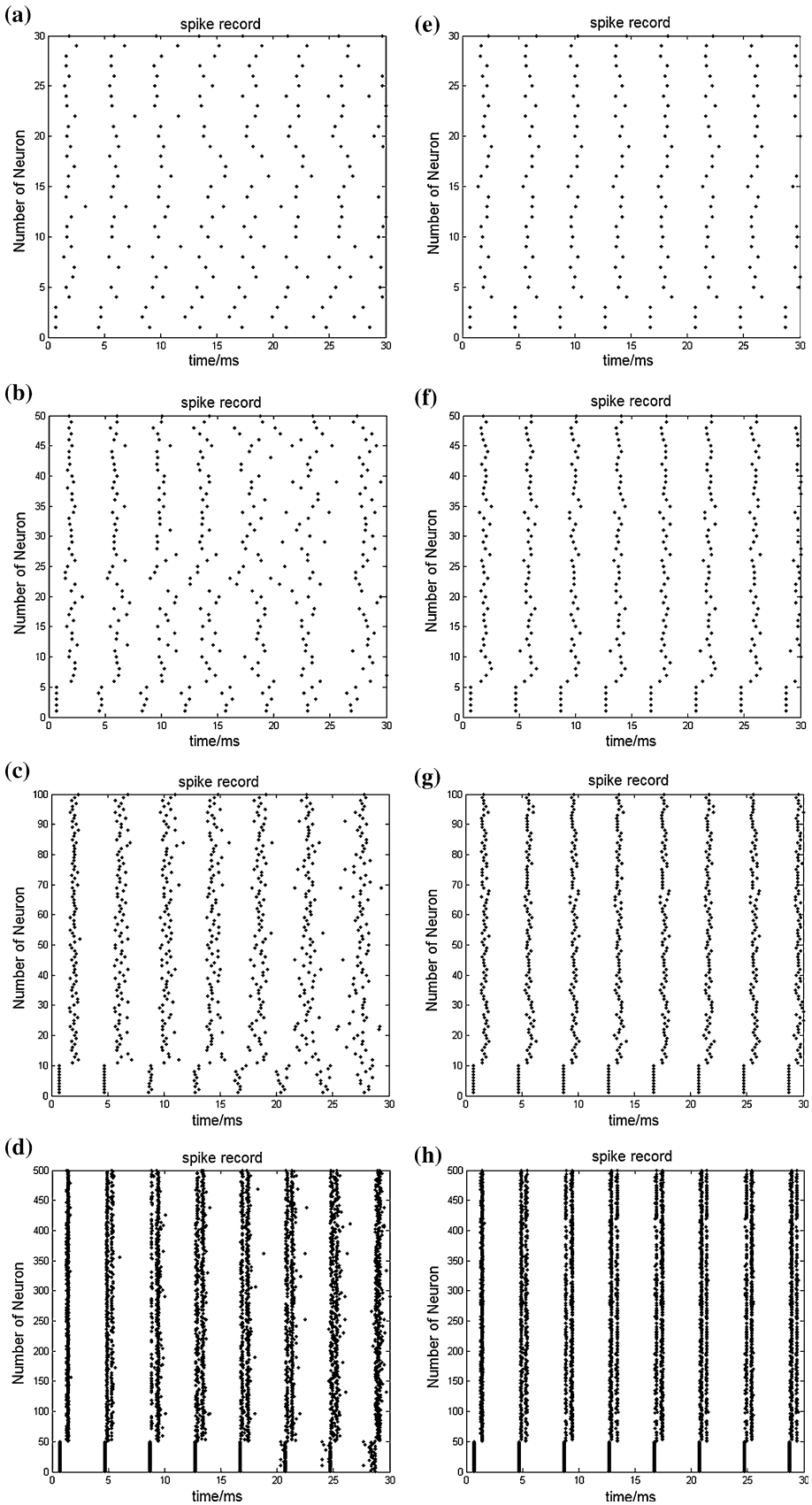

Fig. 7 Nerve impulse record of **a–d** 30 neurons, 50 neurons, 100 neurons and 500 neurons (with inhibitory neurons); Nerve impulse record of **e–h** 30 neurons, 50 neurons, 100 neurons and 500 (without inhibitory neurons) ($a = 0.5 + 0.5 \times \frac{10}{n}$, Coupling strengths between excitatory neurons and the excitation delivery time accord with uniform distribution on the [0, a] and [0.5 ms, 1.5 ms], respectively)

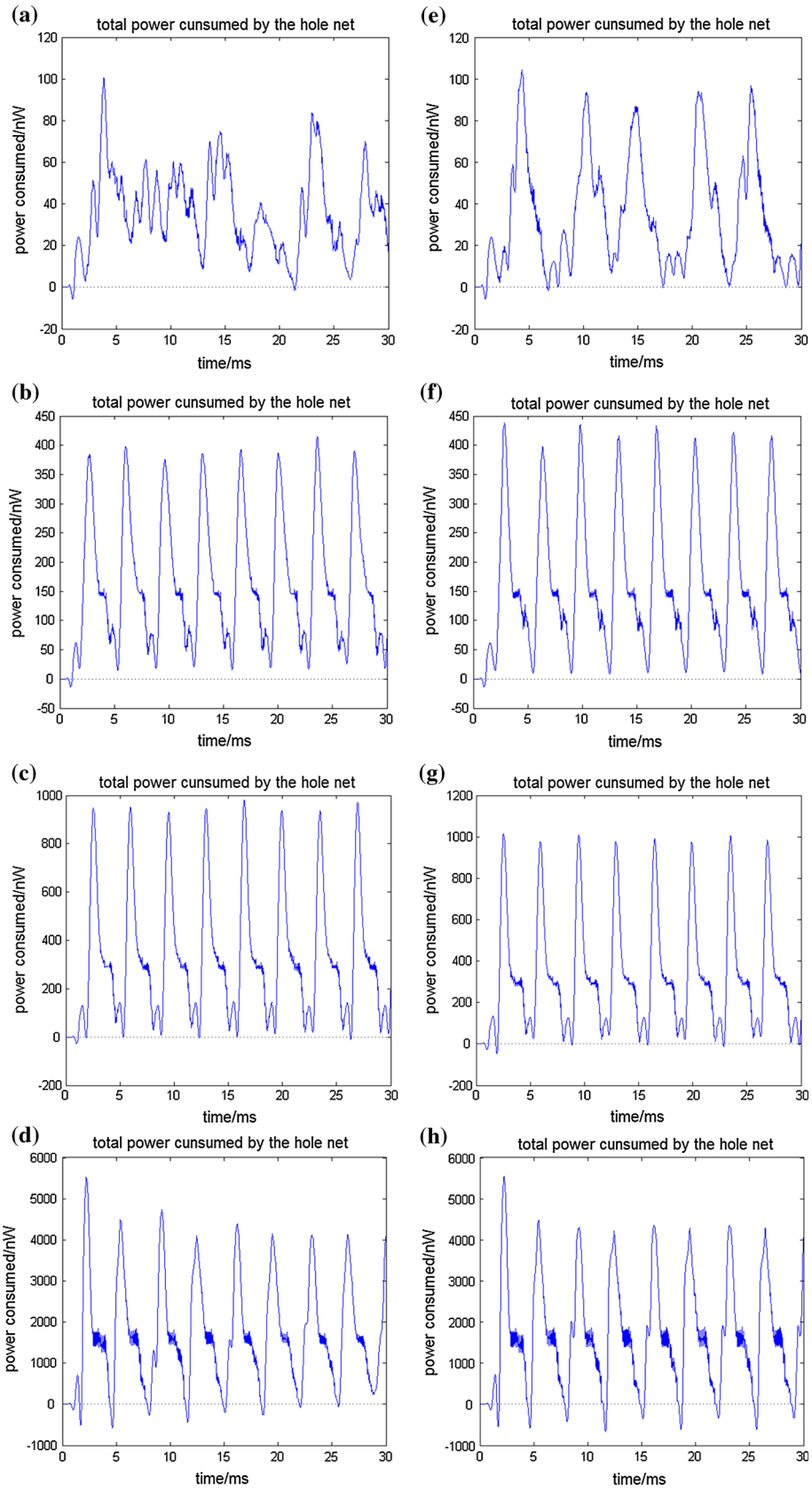

Fig. 8 Total power consumption of **a**–**e** 30 neurons, 50 neurons, 100 neurons and 500 neurons (with inhibitory neurons). **e**–**h** 30 neurons, 50 neurons, 100 neurons and 500 neurons (without inhibitory neurons). ($a = 0.5 + 0.5 \times \frac{10}{n}$, Coupling strengths between excitatory neurons and the excitation delivery time accord with uniform distribution on the [0, a] and [0.5 ms, 1.5 ms], respectively)

Table 2 Simulation results of the network with presence and absence of inhibitory neurons

W/WO inhibitory neurons	Negative energy ratio (%)		Average of maximum correlation coefficient	
	With	Without	With	Without
30	0.0519	0.0572	0.5622	0.6921
50	0.0549	0.0588	0.6636	0.8193
100	0.0648	0.0826	0.8515	0.8533
500	1.2982	1.6286	0.9003	0.9099

Coupling strengths between excitatory neurons and those between inhibitory neurons accord with uniform distribution on the [0, a] and [0, a], respectively, while the excitation delivery time is uniformly distributed on [0.5 ms, 1.5 ms]

which indicating that the regulation of inhibitory neurons reduces synchronization of the overall neuronal impulse firing to a certain extent. Comparing Fig. 7 a–d and b–h, the total power consumption curves, it is seen that with an increase in the number of neurons in a network, the firing synchronization between each neuron is strengthened regardless of the presence or absence of inhibitory neurons, and periodicity of the corresponding total power consumption is also increasingly apparent, which is consistent with the above conclusions.

In order to assess the influence of the inhibitory neurons on the neural network, we performed simulations and got the negative energy ratios and average of the maximum correlation coefficient as shown in Table 2.

From the simulation results in Figs. 7, 8 and Table 2, regardless of neurons number in the network, the pulse firing of the inhibitory neurons induces a relatively large fluctuation of the neuronal membrane potential, and decreases the overall synchronization of the neuronal pulse firing, which results in reduction of the average maximum correlation coefficient in the neuronal population. At the same time, the presence of inhibitory neurons decreases the ratio of negative energy from the total energy.

Though the average of maximum correlation coefficient and negative energy have the same variation trend, the variation of the latter is much more significant than the former. Previous studies have stated that (Wang and Wang 2004) the average of maximum correlation coefficient is only used to characterize the internal oscillation of the neuronal population, while the negative energy ratio can well reflect the oscillations among populations and internal oscillation within populations as well. According to our simulation results, these conclusions remain valid in a network with inhibitory neurons.

Characteristics of coupling strength and power consumption

In the following studies, we fixed the number of neurons in the neural network to be 300, of which we randomly selected 60 neurons as inhibitory neurons and the rest as excitatory neurons. Let $a = 0.5 + 0.5 \times \frac{10}{n}$. We set the coupling strength of excitatory neurons uniformly distributed at [0, a], and adjusted the ratio of the coupling strengths of inhibitory and excitatory neurons. Figures 9a–d shows the pulse firing records within 30 ms in a network comprising 300 neurons, and the coupling strengths of inhibitory neurons were evenly distributed on [0, a], [0, $2a$], [0, $3a$],[0, $4a$], respectively. The corresponding total power consumption curves are shown in Figs. 10a–d.

As can be seen in Fig. 9 that continuous stimulation with intensity of *40 mV* were applied to the first to the thirtieth neurons at time t = 0. After 0.6 ms, these neurons simultaneously fired action potentials and maintained firing periodic pulses.

From Fig. 9, we can clearly see that the firing synchronization of neurons reduces with the increase of coupling strength of inhibitory neurons in the neural network. In images, it is represented as a decline in synchronized firing of dots, and part of dots scatter outside, which indicate that higher coupling strength of inhibitory neurons may induce more significant regulation effects on the pulse firing of other neurons.

From Fig. 10, we observe that with a fixed number of neurons and with increase of coupling strength of the inhibitory neurons in the neuronal population, the periodic trend of the total power consumption reduces, and the ratio of negative energy gradually decreases. Meanwhile, the firing synchronization of the neuron pulse declines as well. Therefore, negative energy ratio can be used to characterize the neural network activity with various coupling strengths of inhibitory neurons. The negative energy ratio and average of maximum correlation coefficient corresponding to Fig. 10 are listed in Table 3.

From results in Fig. 9, 10 and Table 3, we observe that with increasing coupling strength, the periodicity of the total power consumption, ratio of negative energy over total energy, average of maximum correlation coefficient, and synchronization of pulse records show consistent monotonicity. In other words, the total power consumption curves are more likely to present cyclical changes in the steady state, the ratio of negative energy over total energy become smaller, so as the average value of maximum correlation coefficient, and the pulse firing synchronization in the pulse record images become less significant.

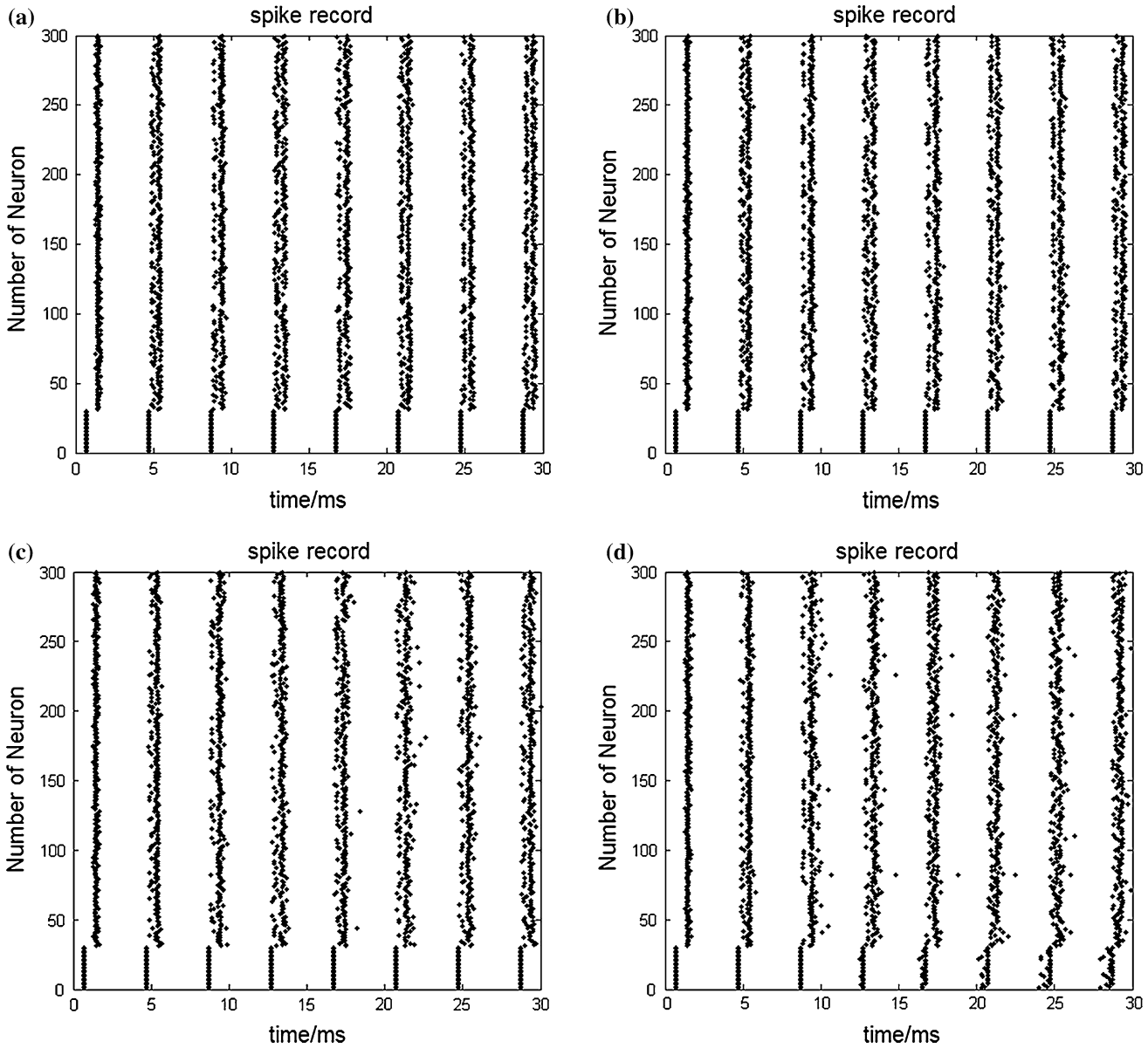

Fig. 9 **a** Nerve impulse record when coupling strengths of inhibitory neurons accord with uniform distribution on [0, a]. **b** Nerve impulse record when coupling strengths of inhibitory neurons accord with uniform distribution on [0, 2a]. **c** Nerve impulse record when coupling strengths of inhibitory neurons accord with uniform distribution on [0, 3a]. **d** Nerve impulse record when coupling strengths of inhibitory neurons accord with uniform distribution on [0, 4a] ($a = 0.5 + 0.5 \times \frac{10}{n}$, Coupling strengths between excitatory neurons and the excitation delivery time accord with uniform distribution on the [0, a] and [0.5 ms, 1.5 ms], respectively)

Relationship between network parameters in neuronal population and energy characteristics

Relationship between quantity of inhibitory neurons and energy characteristics

In order to study the relationship between the energy characteristics and quantity of inhibitory neurons, we developed a neuronal network of 500 neurons and set the excitatory delivery time uniformly distributed on the [0.5 ms, 1.5 ms]. We performed simulations to study the energy distribution with quantity of inhibitory neurons ranged from 0 to 200, and calculated the negative energy ratio and average of maximum correlation coefficient. Their relationships with the quantity of inhibitory neurons are shown in Fig. 11.

Each point in Fig. 11 was obtained by the following rules:

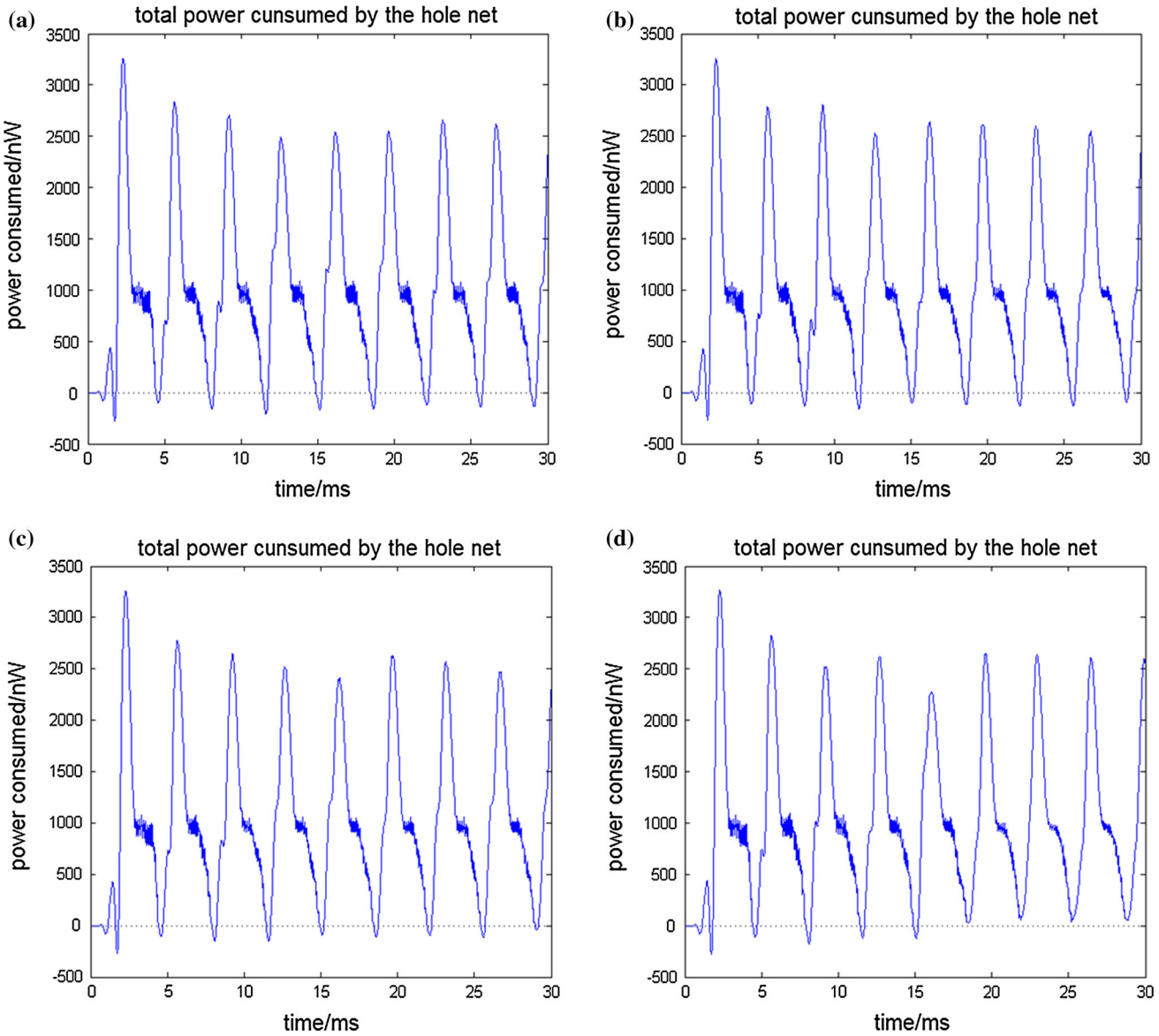

Fig. 10 **a** Total power consumption when coupling strengths of inhibitory neurons accord with uniform distribution on [0, a]. **b** Total power consumption when coupling strengths of inhibitory neurons accord with uniform distribution on [0, 2a]. **c** Total power consumption when coupling strengths of inhibitory neurons accord with uniform distribution on [0, 3a]. **d** Total power consumption when coupling strengths of inhibitory neurons accord with uniform distribution on [0, 4a] ($a = 0.5 + 0.5 \times \frac{10}{n}$, Coupling strengths between excitatory neurons and the excitation delivery time accord with uniform distribution on the [0, a] and [0.5 ms, 1.5 ms], respectively)

1. Let $a = 0.5 + 0.5 \times \frac{10}{n}$. We assumed that coupling strengths of the excitatory neurons and those of the inhibitory neurons were uniformly distributed on the [0, a] and [0, $2a$], respectively.
2. Continuous stimulations were applied to randomly selected 50 neurons in the network with intensity of *40* mV.
3. We conducted simulations to obtain the total power consumption curves of the neuronal population within 30 ms, and calculate the sum by formula 8–12. We repeated the above steps for 10 times, and obtained α_i and $\rho_{meani}(i = 1 \ldots 10)$, and their average value $\bar{\alpha}$ and $\bar{\rho}_{mean}$.
4. The average value was the ordinate value corresponding to current number of neurons in Fig. 11.

As can be seen from Fig. 11, the quantity of inhibitory neurons has a monotonic relationship with the negative energy ratio, which means that more the inhibitory neurons in the neuronal population, the smaller the negative energy ratio. Meanwhile, the average of maximum correlation coefficient maintains the same variation trend with the

Table 3 Negative energy ratio and average of maximum correlation coefficient corresponding to Fig. 10

Coupling strength range of inhibitory neurons	[0, a]	[0, 2a]	[0, 3a]	[0, 4a]
Negative energy ratio (%)	0.8809	0.7527	0.5166	0.3644
Average of maximum correlation coefficient	0.8931	0.8681	0.8657	0.8568

Number of neurons: 300 $a = 0.5 + 0.5 \times \frac{10}{n}$. Coupling strengths between excitatory neurons and the excitation delivery time accord with uniform distribution on the [0, a] and [0.5 ms, 1.5 ms], respectively

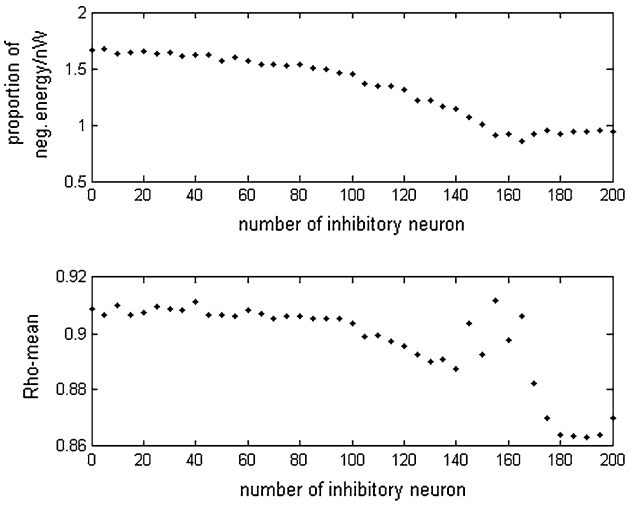

Fig. 11 Negative energy ratio and average of maximum correlation coefficient versus number of inhibitory neurons

negative energy ratio, which indicate that in a network with inhibitory neurons, the neural coding theory based on energy coding also has the capability to characterize network synchronization, and has good agreement with the traditional method of calculating the correlation coefficient. Indeed, quantitative analysis of energy coding is better than the analysis of correlation coefficient. In the above network simulations, when the quantity of inhibitory neurons varied between 0 and 200, the variation range of negative energy ratio was 0.85–1.70, while that of average of maximum correlation coefficient was only 0.860–0.915, indicating that variation of average of maximum correlation coefficient was far less significant than variation of the negative energy ratio. In addition, when the quantity of inhibitory neurons was between 140 and 180, the average of maximum correlation coefficients showed a big fluctuation and was unable to reflect the neural network. In contrast, the negative energy ratio curves were relatively smooth throughout the whole range and could well characterize the situation of the entire network regardless of quantity of inhibitory neurons.

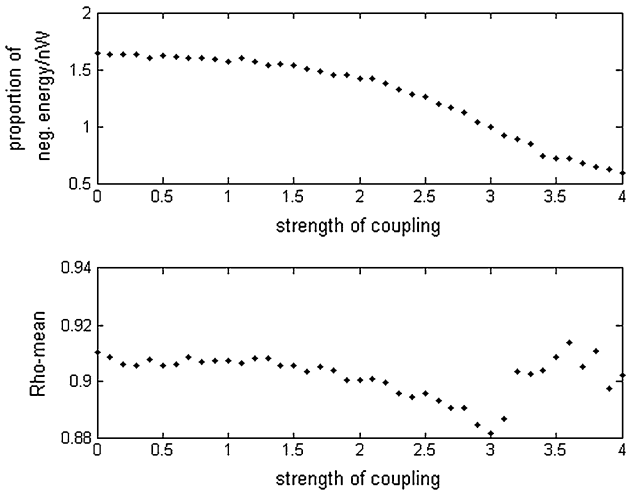

Fig. 12 Negative energy ratio and average of maximum correlation coefficient versus coupling strength of inhibitory neurons. (The horizontal axis represents that the coupling strengths of inhibitory neurons are uniformly distributed on [0, *xa*]

Relationship between coupling strength of inhibitory neurons and neural energy

To study the relationship between the energy characteristics and the coupling strength of inhibitory neurons, we developed a neuronal network of 500 neurons and randomly selected 200 as the inhibitory neurons, and set the excitatory delivery time uniformly distributed at [0.5 ms, 1.5 ms]). We performed simulation to study the total power consumption with different coupling strengths of the inhibitory neurons and calculated the negative energy ratio and average of maximum correlation coefficient. Their relationships with the coupling strength of inhibitory neurons are shown in Fig. 12.

Each point in Fig. 12 was obtained by the following rules:

1. We assumed that the coupling strength of the inhibitory neurons was uniformly distributed on the [0, Δa], Δ varies from 0 through 4 with step 0.1, each one corresponded to one dot in the plot, totally there were 41 dots.
2. We set the number of neurons as 500, and assumed that the coupling strength of the excitatory neurons was uniformly distributed on 40 mV.
3. Continuous stimulations were applied to randomly selected 50 neurons in the network with an intensity of 40 mV.
4. We conducted simulation to obtain the total power consumption curves of the neuronal population within 30 ms, and calculated the sum by Eq. 8–12.
5. Repeated the above steps for 10 times, and obtained α_i and ρ_{meani} ($i = 1 \ldots 10$), and their average value $\bar{\alpha}$ and $\bar{\rho}_{mean}$.

6. The average value was the ordinate value corresponding to current number of neurons in Fig. 12.

We can observe from Fig. 12 that the connecting intensity of inhibitory neurons has a negative correlation with the negative energy ratio, i.e. the greater the coupling strength of inhibitory neurons in the neuronal population, the smaller the negative energy ratio. Meanwhile, the average of maximum correlation coefficient maintains the same variation trend with the negative energy ratio. In the figure, the curve of the negative energy ratio with the coupling strength of the inhibitory neurons is very smooth and can effectively characterize the network conditions with inhibitory neurons of different coupling strengths. However, when the coupling strength reaches above a certain level, the average of maximum correlation coefficient has a larger fluctuation and the value becomes meaningless. The curve is also not smooth when the coupling strength is relatively small. These results indicate that the negative energy ratio can well characterize the difference in neural oscillations caused by changing network parameters.

Conclusion

This paper studied neuronal networks with inhibitory neurons from the energy perspective, and analyzed differences in the synchronous oscillation of the neural network caused by variations of network parameters. It is necessary to emphasize that due to different network models, the actual value of each parameter may be different, but the nature of the intrinsic relationships between them is determined. This suggests that this paper proposes a new method of exploring energy based on synchronous oscillation characteristics between network parameters and network behaviors.

In exploring the total power consumption characteristics in the network oscillations with different parameters, this paper adjusted and changed the parameters such as quantity of neurons and coupling strength of inhibitory neurons in the neuronal population, and found the universal relationship between the network parameters and the total power consumption. In characterizing synchronous oscillation, this paper compared the negative energy ratio and the traditional method of correlation coefficient, and found that the negative energy ratio can better characterize the differences in neural oscillation due to variations of network parameters.

Globally, energy method is a new coding theory for assessing brain activity. One important characteristic of the method is having a superposition feature. In neuroscience experiments, it is very difficult and impossible to record all nerve impulses in a wide areas of the brain, but it is possible to measure the total energy consumption in select regions at different time points. Therefore, the method proposed in this paper is an important supplement to experimental studies. Obviously, this energy method can be used to estimate parameter distributions in brain, and can be easily extended to different parameter distributions in a number of brain regions. Compared with traditional numerical method, this nervous energy coding theory and analysis method has more practical and promotional values.

Acknowledgments This work was supported by the National Natural Science Foundation of China (11232005, 11472104) and the Ministry of Education Doctoral Foundation (20120074110020).

References

Borst A, Theunissen FE (1999) Information theory and neural coding. Nat Neurosci 2(11):947–957

Chadderton P, Schaefer AT, Williams SR, et al (2014) Sensory-evoked synaptic integration in cerebellar and cerebral cortical neurons[J]. Nature Rev Neurosci

Dhamala M et al (2004) Enhancement of neural synchrony by time delay. Phys Rev Lett 92:074104

Feldman J (2013) The neural binding problem(s). Cogn Neurodyn 7(1):1–11

Gazzaniga MS, Ivry RB, Mangun GR (2009) Cognitive neuroscience. The biology of the mind (3rd Edn). Norton & Company, Inc

Ghosh A, Rho Y, McIntosh AR, Kötter R, Jirsa VK (2008) Cortical network dynamics with time delays reveals functional connectivity in the resting brain. Cogn Neurodyn 2(2):115–120

Haken H (2007) Towards a unifying model of neural net activity in the visual cortex. Cogn Neurodyn 1(1):15–25

Igarashi J, Hayashi H, Tateno K (2007) Theta phase coding in a network model of the entorhinal cortex layer II with entorhinal-hippocampal loop connections. Cogn Neurodyn 1(2):169–184

Jacobs AL et al (2009) Ruling out and ruling in neural codes. PNAS 106(14):5936–5941

Johnson DH, Ray W (2004) Optimal stimulus coding by neural populations using rate codes. J Comput Neurosci 16:129–138

Laughlinl SB, Sejnowski TJ (2003) Communication in neural networks. Science. 301:1870

Lin AL, Fox PT, Hardiesa J, Duong TQ, Gao JH (2010) Nonliner coupling between cerebral blood flow, oxygen consumption, and ATP production in human visual cortex. PNAS 107(18):8447

Liu Y, Wang R, Zhang Z, Jiao X (2010) Analysis on stability of neural network in the presence of inhibitory neurons. Congnitive Neurodynamics. 4(1):61–68

McLaughlin David W (2009) Ruling out and ruling in neural codes. Proc Natl Acad Sci PNAS 106(14):5936–5941

Moore CI, Cao R (2008) The hemo-neural hypothesis: on the role of blood flow in information processing. Neurophysiol 99:2035–2047

Nicholls JG, Robert Martin A, Wallace BG (2001) From neuron to brain. Fourth editor. Sinauer Association

Nirenberg S, Latham PE (2003) Decoding neuronal spike trains: how important are correlations? Proc Natl Acad Sci USA 100:7348–7353

Pakhomov A, Sudin N (2013) Thermodynamic view on decision-making process: emotions as a potential power vector of realization of the choice. Cogn Neurodyn 7(3):449–464

Purushothanman G, Bradley DC (2005) Neural population code for fine perceptual decisions in area MT. Nature Neuroscience. 8:99–106

Rokem A, Watzl S, Gollisch T, Stemmler M, Herz AVM, Samengo I (2006) Spike-Timing Precision Underlies the Coding Efficiency of Auditory Receptor Neurons. J Neurophysiol 95:2541–2552

Rubinov M, Sporns O, Thivierge J-P, Breakspear M (2011) Neurobiologically realistic determinants of self-organized criticality in networks of spiking neurons. PLoS Comput Biol 7(6):e1002038

Sokoloff L (2008) The physiological and biochemical bases of functional brain imaging. Cogn Neurodyn 2:1–5

Victor JD (1999) Temporal aspects of neural coding in the retina and lateral geniculate. Network 10:R1–66

Wang Z, Wang R (2004) Energy distribution property and energy coding of a structural neural network. Frontiers in Computational Neuroscience. 8(14):1–17

Wang R, Zhang Z (2006) Mechanism on brain information processing: energy coding. Applied Physical Letters (APL). 89:123903

Wang R, Zhang Z (2007) Energy coding in biological neural network. Cogn Neurodyn 1(3):203–212

Wang R, Zhang Z (2012) Computation of neuronal energy based on information coding. Chinese Journal of Theoretical and Applied Mechanics. 44(4):779–786

Wang R, Wang Z, Tsuda I (2004) A new mechanism of neuronal activity. Int J Neural Sys

Wang R, Zhang Z, Chen G (2008) Energy function and energy evolution on neural population. IEEE Trans Neural Networks 19(3):535–538

Wang R, Zhang Z, Chen G (2009) Energy coding and energy functions for local activities of brain. Neurocomputing. 73(1–3):139–150

Xie J, Wang Z (2013) Effect of inhibitory feedback on correlated firing of spirking neural netwaor. Congnitive Neurodynamics. 7:4